11-2013

Magnetocaloric and Magnetic Properties of $Ni_2Mn_{1-x}Cu_xGa$ Heusler Alloys: an Insight from the Direct Measurements and *ab initio* and Monte Carlo Calculations

V. Sokolovskiy

V. Buchelnikov

K. Skokov

O. Gutfleisch

D. Karpenkov

See next page for additional authors

Published in *Journal of Applied Physics*, Vol. 114 No. 183913 (2013) at doi: 10.1063/1.4826366

Magnetocaloric and magnetic properties of $Ni_2Mn_{1-x}Cu_xGa$ Heusler alloys: An insight from the direct measurements and *ab initio* and Monte Carlo calculations

V. Sokolovskiy,[1,2,a)] V. Buchelnikov,[1] K. Skokov,[3] O. Gutfleisch,[3] D. Karpenkov,[4] Yu. Koshkid'ko,[4] H. Miki,[5] I. Dubenko,[6] N. Ali,[6] S. Stadler,[7] and V. Khovaylo[2]
[1]*Faculty of Physics, Chelyabinsk State University, Chelyabinsk 454001, Russia*
[2]*Institute of New Materials and Nanotechnology, National University of Science and Technology "MIS&S," Moscow 119049, Russia*
[3]*Institut für Materialwissenschaft, Technische Universität Darmstadt, Darmstadt 64287, Germany*
[4]*Faculty of Physics, Tver State University, Tver 170000, Russia*
[5]*Institute of Fluid Science, Tohoku University, Sendai 980-8577, Japan*
[6]*Department of Physics, Southern Illinois University, Carbondale, Illinois 62901, USA*
[7]*Department of Physics and Astronomy, Louisiana State University, Baton Rouge, Louisiana 70803, USA*

(Received 26 June 2013; accepted 6 October 2013; published online 14 November 2013)

We calculated magnetic exchange constants and magnetocaloric properties of $Ni_2Mn_{1-x}Cu_xGa$ Heusler alloys by *ab initio* and Monte Carlo methods. The *ab initio* study of the influence of the Cu excess x on the strength of magnetic interactions revealed that Cu weakens Mn-Ni interaction and has a complex impact on the Mn-Mn interactions. Theoretically calculated magnetic phase diagram of $Ni_2Mn_{1-x}Cu_xGa$ is in a good agreement with available experimental data. Calculated by the Monte Carlo method the isothermal magnetic entropy change ΔS_{mag} in a $Ni_2Mn_{0.75}Cu_{0.25}Ga$ alloy is significantly smaller around the coupled magnetostructural phase transition temperature than the reported earlier experimental ΔS_{mag}. This discrepancy is ascribed to an overestimation of the experimental ΔS_{mag} at the magnetostructural phase transition. Theoretically determined adiabatic temperature change ΔT_{ad} in $Ni_2Mn_{0.75}Cu_{0.25}Ga$ agrees well with ΔT_{ad} measured experimentally by a direct method. © *2013 AIP Publishing LLC*. [http://dx.doi.org/10.1063/1.4826366]

I. INTRODUCTION

Today, great efforts have been devoted to the search for ferromagnetic materials suitable for application as refrigerants in the magnetic cooling devices.[1] Performance of these devices is substantially conditioned by the magnetocaloric effect (MCE) of a refrigerant. The essential characteristics of MCE are adiabatic temperature change ΔT_{ad} and isothermal magnetic entropy change ΔS_{mag} which occur in any magnetic material upon action of an external magnetic field. In magnetically ordered substances undergoing conventional second order magnetic phase transitions the MCE reaches its maximal value at the magnetic ordering temperature.[2] In the temperature range of interest for commercial refrigeration, this so-called ordinary MCE is most pronounced in rare-earth elements and alloys,[3] specifically in Gadolinium, which has been considered as a prototypical material for the room-temperature magnetic refrigeration technology.[4]

Some of the intermetallic alloys and compounds were reported recently to exhibit an enhanced, or giant, magnetocaloric effect in the vicinity of room temperature. These include Gd(Si,Ge), La(Fe,Si), MnAs, MnFe(P,As), and NiMnX (X = Ga, In, Sn, Sb) systems.[5–7] In all these alloys the enhancement of MCE is observed near first order magnetostructural phase transition temperature, where magnetic and structural (or isostructural) phase transitions occur simultaneously. Since the magnetostructural phase transitions are accompanied by a rapid change of the magnetization with temperature, the systems with such transitions are reported to exhibit the isothermal magnetic entropy change greatly exceeding that of Gd, i.e., are referred to as giant MCE materials. Especially large ΔS_{mag} has been declared for practically all members of the Heusler-based NiMnX ferromagnetic shape memory alloys. Since the system with X = Ga is the most studied among the NiMnX family of Heusler alloys, a throughout examination of magnetocaloric and magnetic properties of a NiMnGa-based representative of ferromagnetic shape memory alloys is worth performing from both fundamental and technological points of view.

The stoichiometric Ni_2MnGa alloy undergoes a structural transformation from the parent austenitic to a product martensitic phase on cooling below $T_m \approx 200$ K while a ferromagnetic ordering in this compound sets at a sufficiently higher temperature $T_C = 376$ K.[8] Both the martensitic transformation temperature T_m and the Curie temperature T_C were found to depend strongly on stoichiometry[9,10] as well as on alloying.[11–13] For example, recent experimental studies of $Ni_{2+x}Mn_{1-x}Ga$ alloy series have shown that an increase of the Ni excess leads to an increase of the martensitic transformation temperature T_m whereas the Curie temperature T_C shows a tendency to decrease with the deviation from the stoichiometry.[14] In a concentration interval $0.18 \leq x \leq 0.27$ the structural and the magnetic phase transition merge, i.e., these alloys undergo a coupled first order magnetostructural phase transition from ferromagnetic martensite to paramagnetic austenite. Judging by the reported value of isothermal magnetic entropy change,[15] these alloys are representative of

a)Electronic mail: vsokolovsky84@mail.ru

giant MCE materials though their adiabatic temperature change measured experimentally by a direct method[16,17] turned our to be comparable with that of Gd.

Among NiMnGa-based alloys, one of the record values of the isothermal magnetic entropy change has been reported for Cu-doped samples.[18–22] The earliest systematic study of Cu-containing NiMnGa showed that addition of Cu on Ni site rapidly suppresses martensitic transformation in $Ni_{2-x}Cu_xMnGa$ which disappears for the $x=0.1$ composition.[23] When nominal content of Ni is kept stoichiometric in Ni_2MnGa, the addition of Cu to this ternary Heusler compound allows one to smoothly adjust both magnetic and structural transition temperatures[24–26] or brings about an uncommon transformation sequence from low-temperature non-magnetic martensite to high-temperature ferromagnetic austenite.[27] Systematic studies of magnetic and structural phase transitions in Cu-doped Ni_2MnGa revealed striking similarity of the phase diagrams of $Ni_2Mn_{1-x}Cu_xGa$ (Ref. 28) and $Ni_{2+x}Mn_{1-x}Ga$.[14] In the sense T_m and T_C tendencies, the addition of Cu in $Ni_2Mn_{1-x}Cu_xGa$ and the substitution of Mn for Ni in $Ni_{2+x}Mn_{1-x}Ga$ have an identical effect. As in the case of $Ni_{2+x}Mn_{1-x}Ga$, the phase transitions in $Ni_2Mn_{1-x}Cu_xGa$ merge in a rather extended range of compositions, from $x=0.23$ to $x=0.30$.[28] Results of x-ray absorption spectroscopy and x-ray magnetic circular dichroism suggest[29] that Cu has a complex impact on the magnetic and structural subsystems of the parent compound. On one hand, Cu weakens magnetic interactions which brings about a decrease in the Curie temperature T_C. On the other hand, alloying with Cu reinforces Ni covalency thus strengthening Ni-Ga chemical bonds which is accompanied by a rise of martensitic transition temperature.[30]

In $Ni_2Mn_{1-x}Cu_xGa$, the magnetostructural transition occurs just above room temperature, e.g., at $T_m \approx 308$ K for the $x=0.25$ composition,[18] and this transition temperature can be tuned through a subtle variation of the Cu concentration[28] or Mn stoichiometry.[22] In a recent study, a giant MCE with $\Delta S_{mag} \approx -64$ J/(kgK) for the magnetic field change of 5 T has been reported in $Ni_2Mn_{0.75}Cu_{0.25}Ga$ at 308 K.[18] This temperature is very suitable for the purpose of the room-temperature magnetic refrigeration. Moreover, T_m can easily be adjusted by a minor change in the chemical composition of the material.[18,19,22,28] Thus, there is a strong motivation for a detailed investigation of MCE and magnetic properties of the $Ni_2Mn_{1-x}Cu_xGa$ alloys.

In the present work we report on experimental and theoretical studies of magnetocaloric effect and the exchange interactions in $Ni_2Mn_{1-x}Cu_xGa$ Heusler alloys by the direct measurements of MCE and the *ab initio* and Monte Carlo calculations. We employ first-principles electronic structure calculations in conjunction with a Heisenberg model to compute the sublattice specific pairwise exchange interactions. The knowledge of the exchange interactions in $Ni_2Mn_{1-x}Cu_xGa$ helps to construct, both qualitatively and quantitatively, a correct picture of the magnetic interactions in this system. Also, it allows one to track the trends in magnetization and to calculate the main characteristics of MCE which then can be compared with the experimentally measured ones.

The paper is organized as follow. Section II is devoted to the description of the measurement technique and the experimental results obtained. In Sec. III we present the *ab initio* calculation approach and some results on exchange interactions in austenitic and martensitic phase of $Ni_2Mn_{1-x}Cu_xGa$. The Monte Carlo theoretical model is described in Sec. IV. In Sec. V, this model is utilized to calculate isothermal magnetic entropy change and adiabatic temperature change in $Ni_2Mn_{0.75}Cu_{0.25}Ga$. Concluding remarks are given in Sec. VI.

II. DIRECT MEASUREMENTS OF MCE IN $Ni_2Mn_{0.75}Cu_{0.25}Ga$

The $Ni_2Mn_{0.75}Cu_{0.25}Ga$ sample used for experimental measurements of MCE by a direct method was cut from a polycrystalline ingot which was prepared by a conventional arc-melting method and annealed at 1073 K for 6 days in a vacuum furnace.[18] Structural, magnetic, and magnetocaloric (ΔS_{mag} for the magnetic field change up to 5 T) properties of this alloy have been were reported earlier.[18]

Direct measurements of the adiabatic temperature change ΔT_{ad} were performed by an experimental setup described in Ref. 31. Permanent magnets arrayed in the Halbach cylindrical configuration produced magnetic field up to maximal strength 1.93 T in the bore center. Sweep rate of the magnetic field was 2 T/s. The temperature of the sample was monitored with accuracy better than 0.02 K by a Copper-Constantan thermocouple which was in a good thermal contact with the sample. ΔT_{ad} was measured at fixed temperatures upon warming up (heating protocol) and cooling down (cooling protocol). During the measurement procedure, the target temperature was approached without overheating/overcooling. Temperature of the sample was well stabilized prior to the application of the magnetic field.

Temperature dependencies of ΔT_{ad} measured upon heating and cooling are shown in Fig. 1. It is seen that the adiabatic temperature change exhibits a peak with a maximal value $\Delta T_{ad} \approx 0.75$ K at 305 K upon heating and $\Delta T_{ad} \approx 1.5$ K at 303 K upon cooling. A hysteresis in the

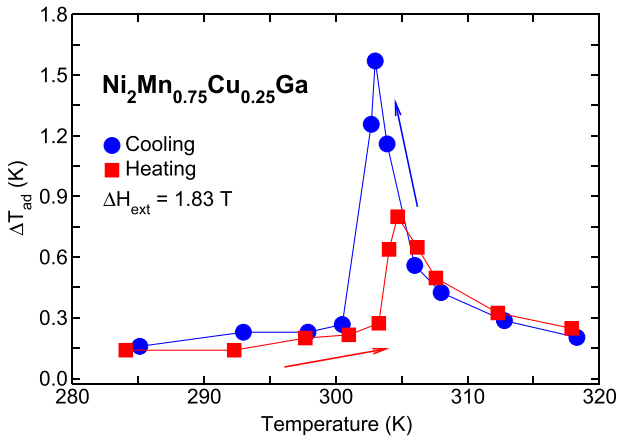

FIG. 1. Adiabatic temperature change ΔT_{ad} measured for a $Ni_2Mn_{0.75}Cu_{0.25}Ga$ alloy upon heating (squares) and cooling (circles) in the vicinity of the magnetostructural transition. The solid lines are a guide for the eyes.

peak position is due to a first order character of the magneto-structural phase transition.[18] It is worth mentioning a twofold difference in the maximal value of ΔT_{ad} measured upon heating and cooling protocol. This is caused by a specific response of the system to the application of an external magnetic field that depends on the measurement protocol. Particularly, for the magnetic fields used in the present study the magnetic field-induced transformation, hence an additional contribution to ΔT_{ad} from the structural subsystem, can be realized in conventional ferromagnetic shape memory alloys like Ni-Mn-Ga or Ni-Mn(Cu)-Ga only upon cooling protocol. This is due to a large difference in the magnetic field strength sufficient to induce martensitic transformation upon heating and cooling protocol.[32] Note that opposite situation is observed in metamagnetic shape memory alloys like Ni-Mn-In or Ni-Mn-Sn.[33]

III. *AB INITIO* CALCULATION OF EXCHANGE INTERACTIONS IN $Ni_2Mn_{1-x}Cu_xGa$

To perform calculations of the electronic structure and the exchange interactions in a real space, we have used the Spin Polarized Relativistic Korringa-Kohn-Rostoker (SPR-KKR) method.[34] This code is based on the Green's functions as opposed to Bloch wave functions and eigenvalues. The Heisenberg exchange parameters were calculated using the theory of Lichtenstein *et al.*,[35] where the exchange interactions between a pair of J_{ij} spins is calculated using a classical Heisenberg Hamiltonian. In this method, the exchange parameters were computed from the total energy variation caused by small rotations of a pair of spins.

The effect of chemical disorder on J_{ij} was taken into account using a single-site coherent potential approximation (CPA). The maximum number of CPA iterations and a CPA tolerance were set to 20 and 0.01 mRy, respectively. The first step in these calculations is to calculate the self-consistent potential (SCF). The angular momentum expansion for the major component of the wave function, l_{max}, was restricted to two. For SCF cycles, the scattering path operator was calculated by the Brilloiun-zone (BZ) integration[36] with the special point method using a regular k-mesh grid of 22^3 with 834 k-points. All calculations were converged to 0.01 mRy of the total energy. To achieve this convergence, we have used a BROYDEN2 scheme[37–39] with Vosko-Wilk-Nusair (VWN) exchange-correlation potential.[40] The BROYDEN2 scheme was started after the first iteration. The iteration depth for the BROYDEN algorithm was set to 40. For the SCF calculations, an arc-like contour path in the complex energy plane has been chosen as approach to weakly bound states which are treated as the core states. The upper end of the energy path E_{max} is set to the Fermi energy E_F. Regarding the real part of the lowest energy value, E_{min}, we have used a value of $E_{min} = -0.2$ Ry. The number of E-mesh points was set to 30. In order to achieve faster convergence, the SCF mixing parameter was set to 0.20. The maximum number of SCF iterations was taken to 200. The self-consistent potential is then used to calculate the magnetic exchange parameters with the help of the KKR Green's function method and the approach of Liechtenstein *et al.*[35] For this aim, the spin-polarized scalar-relativistic (SP-SREL) Dirac Hamiltonian with an orbital momentum cutoff of $l_{max} = 2$ on a grid of 57^3, i.e., 4495 k-points, has been taken. As a solver for SP-SREL differential equations, the Bulirsch-Stoer (BS) method[39] with a tolerance of 2×10^{-8} was used. The exchange coupling parameters have been calculated with respect to the central site i of a cluster of atoms with a radius $R_{clu} = \max|R_i - R_j|$. In our calculations, this radius was taken as $R_{clu} = 2.0$.

Experimental studies of crystal structure of NiMn-based Heusler alloys have shown that a high-temperature austenite phase has $L2_1$ cubic structure. The low-temperature martensite phase can be either modulated with monoclinic (or orthorhombic) symmetry or tetragonal non-modulated, depending on the chemical composition which is related to the average valence electron concentration e/a.[9,10] In 1991, Khachaturyan *et al.*[41] suggested that modulated martensitic structures can be considered as a tetragonal structure having a high density of ordered nanotwins. Later on, this adaptive modulation concept has been applied for the case of NiMn-based ferromagnetic shape memory alloys.[42,43] Following this approach, in our simulations we shall treat the low-temperature phase of $Ni_2Mn_{1-x}Cu_xGa$ as a tetragonal one. Since determination of the crystallographic parameters from the first principles is not the primary target of this work, in our calculations the crystal lattice parameter of the cubic austenite and the crystallographic distortion of the tetragonal martensite were taken from the available experimental data[28] as $a = 0.579$ nm and $c/a = 1.147$, respectively. For quaternary $Ni_2Mn_{1-x}Cu_xGa$ alloys, we consider that the Cu atoms occupy the Mn sublattice. The Wyckoff positions of the atoms in the austenite and the martensite are given in Table I.

Figure 2 shows composition dependencies of the magnetic exchange integrals of $Ni_2Mn_{1-x}Cu_xGa$ in the first, second, and third coordination spheres for the cubic $L2_1$ and tetragonal $L1_0$ structures. As is seen from Fig. 2, for compositions with a low concentration of Cu atoms the Mn-Ni interaction in the first coordination sphere is positive and slightly stronger in the martensitic state than in the austenitic one. The increase of the Cu excess leads to a decrease of the interaction strength between Mn and Ni atoms. The Mn-Ni interaction in the second and third coordination spheres in both austenite and martensite are virtually absent. Also, one can notice that the Mn-Cu interaction in all three coordination spheres is negligible in both the structures (Fig. 2).

Contrary to the Mn-Ni and Mn-Mn interactions, the Mn-Mn interaction demonstrates a drastic difference in the

TABLE I. Atomic positions in austenite and martensite of $Ni_2Mn_{1-x}Cu_xGa$ alloys.

Elements	$(c/a = 1)$[a]	$(c/a = 1.147)$[b]
Ni	8c: 0.25; 0.25; 0.25	8f: 0.25; 0.25; 0.25
Mn	4b: 0.5; 0.5; 0.5	4b: 0; 0; 0.5
Ga	4a: 0; 0; 0	4a: 0; 0; 0
Cu	4b: 0.5; 0.5; 0.5	4b: 0; 0; 0.5

[a]Austenite.
[b]Martensite.

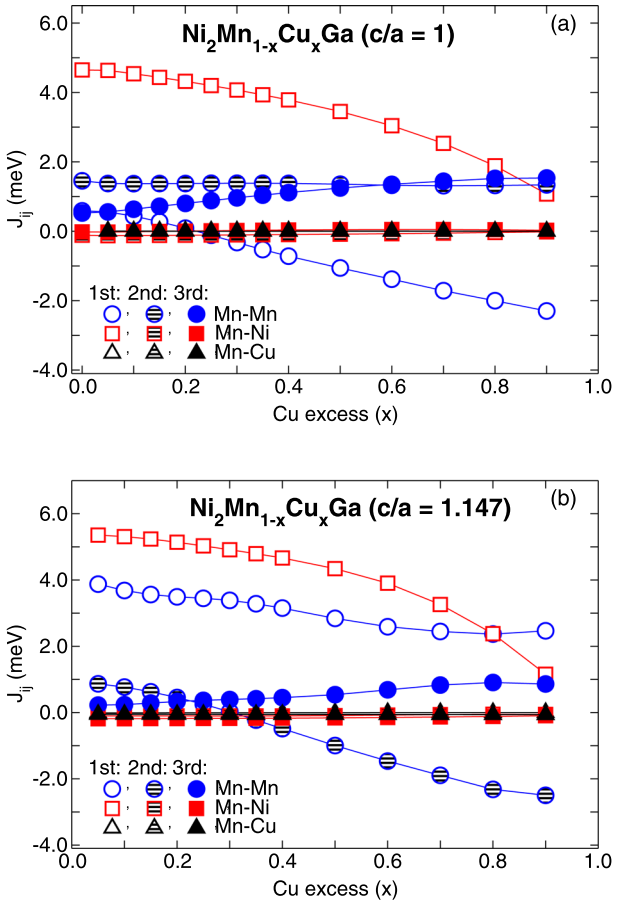

FIG. 2. *Ab initio* magnetic exchange interactions of $Ni_2Mn_{1-x}Cu_xGa$ for the (a) cubic ($c/a = 1$) and (b) tetragonal ($c/a = 1.147$) phase as a function of the Cu excess x. Here the lines with open (line filled, and filled) symbols are interaction in the first (second, and third) coordination sphere, respectively. The circle (triangle, and square) symbols denote the Mn-Mn (Mn-Cu, and Mn-Ni) interactions, respectively.

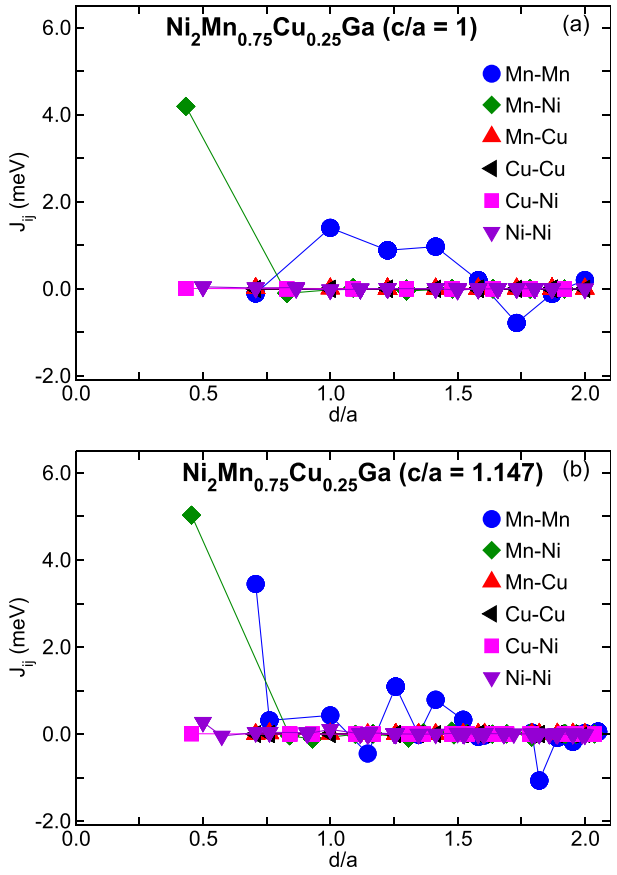

FIG. 3. *Ab initio* magnetic exchange interactions of $Ni_2Cu_{0.25}Mn_{0.75}Ga$ in the (a) cubic ($c/a = 1$) and (b) tetragonal ($c/a = 1.147$) state as a function of the distance between atoms. Here d/a is a distance between pairs of atoms i and j (in units of the lattice constant a).

austenitic and martensitic state. In the austenitic state the Mn-Mn interaction in the first coordination sphere is rather weak and changes its sign from positive to negative at $x \approx 0.22$ (Fig. 2(a)) whereas in the martensitic state this interaction plays a dominate role in determining ferromagnetic properties of the low-temperature phase (Fig. 2(b)). The Mn-Mn interactions in the second and third coordination spheres are ferromagnetic in the austenitic state, and in the compositions with $x \geq 0.5$ these interactions are approximately of the same strength (Fig. 2(a)). In the martensitic state the Mn-Mn interactions in the second and third coordination spheres demonstrate opposite trends with the increase of the Cu excess x. Specifically, the Mn-Mn interaction in the second coordination sphere is positive and decreases as x increases while that in the third coordination sphere is negative and linearly increases with the increase of the Cu excess x. Both the interactions change sign (from positive to negative in the second coordination sphere and from negative to positive in the third one) in a composition with $x \approx 0.6$ (Fig. 2(b)).

The magnetic exchange integrals of $Ni_2Cu_{0.25}Mn_{0.75}Ga$ in the cubic and tetragonal phase are presented in Fig. 3 as a function of the distance between atoms in the units of the lattice constant a. It can be seen from Fig. 3 that except the Mn-Ni interaction in the first coordination sphere and the Mn-Mn interactions, the rest of the interactions (Cu-Cu, Cu-Ni, and Cu-Mn) are negligible. In both the phases, the Mn-Mn interactions show a long-range oscillatory behavior. In the cubic austenitic phase the Mn-Mn interaction in the first coordination sphere is weaker than that in the following ones. In the first five coordination spheres the Mn-Mn interaction is ferromagnetic but becomes antiferromagnetic in the sixth coordination sphere (Fig. 3(a)). In the tetragonal martensitic state, the oscillatory behavior of the Mn-Mn interaction is even more pronounced (Fig. 3(b)). Approximately the same behavior of the Mn-Mn interaction has been observed early in the works.[44,45]

The Curie temperatures of austenitic and martensitic phases were calculated within the mean-field approximation of the Heisenberg model for a multisublattice material by solving a system of coupled equations[44]

$$\langle s^{\mu} \rangle = \frac{2}{3k_B T} \sum J_0^{\mu\nu} \langle s^{\nu} \rangle. \quad (1)$$

Here $J_0^{\mu\nu} = \sum_{\mathbf{R}} J_{0\mathbf{R}}^{\mu\nu}$ is the total magnetic exchange parameter between an atom at site μ and its neighbor at site ν, $\mathbf{R}$ is the lattice vector specifying the atoms within sublattice, $\langle s^{\mu} \rangle$ is the average z component of $s_{\mathbf{R}}^{\mu}$ (the unit vector pointing in the direction of the magnetic moment at site $(\mu, \mathbf{R})$), and k_B is the Boltzmann constant.

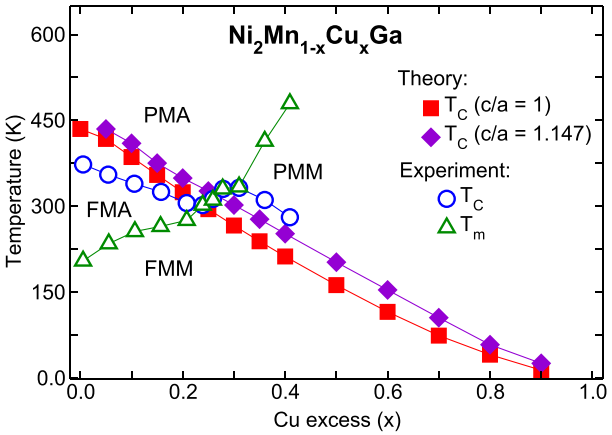

FIG. 4. Theoretical and experimental $T - x$ phase diagrams for $Ni_2Mn_{1-x}Cu_xGa$. Theoretical Curie temperatures for the austenitic and martensitic phases are calculated using mean-field approximation. Here, T_C and T_m are the Curie temperature and the temperature of martensitic transformation, FMM (PMM) and FMA (PMA) are the ferromagnetic (paramagnetic) martensite (austenite), respectively. Experimental data are taken from Ref. 28.

This equation has non-trivial solutions if the corresponding determinant is zero, viz.,

$$Det\{\Theta - T\mathbf{I}\} = 0; \Theta_{\mu\nu} = \frac{2}{3k_BT}\sum J_0^{\mu\nu}, \tag{2}$$

where $\mathbf{I}$ is a unit matrix. The largest eigenvalue of matrix gives the value of the Curie temperature.

Figure 4 shows compositional dependencies of T_C for the $L2_1$ and $L1_0$ phases calculated from the Heisenberg model using the mean-field approximation. One can see that the increase in the Cu excess x leads to a decrease in T_C of both the phases and that T_C in the martensitic phase is larger than that in the austenitic phase. Experimental studies of $Ni_2Mn_{1-x}Cu_xGa$ revealed[28] that upon substitution of Mn for Cu the Curie temperature T_C decreases whereas the martensitic transformation temperature T_m increases until they merge in a $Ni_2Mn_{0.78}Cu_{0.22}Ga$ composition. A coupled magnetostructural phase transition ferromagnetic martensite paramagnetic austenite is observed in a compositional range $0.22 \le x \le 0.3$. In alloys with $x > 0.3$ the magnetic and structural transitions decouple in such a way that $T_C < T_m$. It is clear therefore that the magnetic transition in the alloys with $0.0 \le x \le 0.22$ corresponds to the Curie temperature of austenite whereas that in the alloys with $x \ge 0.3$ is Curie temperature of the martensitic phase. As can be seen from Fig. 4, value and compositional dependence of theoretically calculated Curie temperature of the martensitic phase is in a fair quantitative and a good qualitative agreement with T_C determined experimentally. For the Curie temperature of austenite, both theoretical calculation and experimental studies[28] showed that T_C decreases almost linearly with the increase of Cu excess x. However, experimentally determined decrease of T_C is less pronounced than that obtained theoretically.

IV. THEORETICAL LATTICE MODEL

Proposed theoretical Monte Carlo (MC) model takes into account magnetic and elastic interactions on the three-dimensional lattice with the real unit cell of Ni-Mn-Ga Heusler alloys. The cubic $L2_1$ structure consists of four interpenetrating fcc sublattices with Mn at site (1/2, 1/2, 1/2), Ga at site (0, 0, 0), and Ni at sites (1/4, 1/4, 1/4) and (3/4, 3/4, 3/4), respectively.[8] In the present model we consider only two martensitic variants in the low-temperature tetragonal state instead of six structural variants. In the case of non-stoichiometric $Ni_2Cu_{0.25}Mn_{0.75}Ga$ alloy, the Cu atoms are located at regular Mn positions. The *ab initio* calculations of magnetic exchange constants show that Mn-Ni interaction is positive (see Fig. 3). Moreover it is the largest of all exchange integrals, in spite of the fact that the magnetic moment of the Ni atoms is much smaller than the magnetic moment of Mn atoms. The *ab initio* calculations have also shown that the magnetic interactions between Cu and Mn (Ni) atoms are negligible. Therefore in our simulations we consider that the Cu atoms are non-magnetic atoms as the Ga atoms. So, the Mn and Ni atoms have magnetic and structural degrees of freedom whereas the sites occupied by Ga and Cu atoms have only structural degrees of freedom. Hence, the whole system can again be considered as consisting of interacting magnetic and structural subsystems.

The full Hamiltonian consists of three contributions[45,46]

$$\mathcal{H} = \mathcal{H}_m + \mathcal{H}_{el} + \mathcal{H}_{int}. \tag{3}$$

The magnetic part H_m is described by a 3-6-state Potts model as

$$\mathcal{H}_m = -\sum_{\langle i,j\rangle}^{NN} J_{i,j}^m \delta_{S_i,S_j} - g\mu_B H_{ext}\sum_i^N \delta_{S_i,S_g}. \tag{4}$$

Here, 3 and 6 corresponds to the maximal number of Ni and Mn spin states, respectively. Note that in previous calculations[45,46] the 3–5 states Potts model was used where the spin moments S with $2S + 1$ spin projections of Ni $(-1, 0, 1)$ and Mn $(-2, -1, 0, 1, 2)$ were characterized by Potts states $q_{Ni} = 3$ and $q_{Mn} = 5$, respectively. However, Kimura *et al.*[47] observed that in Mn-based magnetic intermetallic compounds, specifically in Heusler alloys, the ferromagnetic moment of Mn atoms is characterized by a Mn^{2+} form factor which corresponds to the spin value 5/2 with spin projections $(-5/2, -3/2, -1/2, 1/2, 3/2, 5/2)$. Therefore, in this work we use the 3-6 states Potts model with $q_{Mn} = 6$ for the Mn atoms instead of $q_{Mn} = 5$. Although the difference between both models is minimal, Monte Carlo simulations of magnetic properties and MCE show, while the magnetization $m(T)$ changes to be slightly stronger near structural and magnetic phase transitions.

The structural part H_{el} is described by a degenerate Blume-Emery-Griffiths (BEG) model

$$\mathcal{H}_{el} = -J\sum_{\langle i,j\rangle}^{NN}\sigma_i\sigma_j - K\sum_{\langle i,j\rangle}^{NN}(1-\sigma_i^2)(1-\sigma_j^2) - k_BT\ln(p)\sum_i^N(1-\sigma_i^2) - K_1 g\mu_B H_{ext}\sum_i^N \delta_{\sigma_g\sigma_j}\sum_{\langle i,j\rangle}^{NN}\sigma_i\sigma_j, \tag{5}$$

and the magnetostructural interaction H_{int} is defined as

$$\mathcal{H}_{int} = 2\sum_{\langle i,j\rangle}^{NN} U_{i,j}\delta_{S_i,S_j}\left(\frac{1}{2}-\sigma_i^2\right)\left(\frac{1}{2}-\sigma_j^2\right) - \frac{1}{2}\sum_{\langle i,j\rangle}^{NN} U_{i,j}\delta_{S_i,S_j}. \tag{6}$$

Here, $J_{i,j}^m$ is the magnetic exchange parameter which may become negative depending on the degree of tetragonal distortion or disorder. S_i is a spin defined on the lattice site $i = 1\ldots N$. The Kronecker symbol, $\delta_{Si,Sj}$, restricts spin-spin interactions to the interactions between the same q_{Mn} states of Mn and q_{Ni} states for Ni atoms, where q_{Ni} and q_{Mn} are the numbers of magnetic states of Ni and Mn atoms, respectively. For the Ni and Mn atoms we have three spin states $(-1, 0, 1)$ and six spin states $(-5/2, -3/2, -1/2, 1/2, 3/2, 5/2)$, respectively.[45–47] The other Kronecker symbol, $\delta_{Si,Sg}$, couples the spin system to the external magnetic field H_{ext}, S_g is called a ghost spin,[45,46] its impact is that positive H_{ext} favors spin parallel to the ghost spin S_g. μ_B is Bohr's magneton, and g is the Landé factor. J and K are "structural exchange" constants for tetragonal and cubic states, respectively. The variable $\sigma_i = 1, 0, -1$ defines the deformation state near each lattice site. p is a degeneracy factor that characterizes the number of structural variants. The states $\sigma_i = \pm 1$, and 0 represent the tetragonal and cubic phase, respectively. K_1 is the dimensionless magnetoelastic interaction constant. σ_g is a *ghost deformation state*, characterized by the structural variant which is favored in an external magnetic field.[45,46] T is the temperature and k_B the Boltzmann constant, U_{ij} is magnetoelastic interaction parameter. The summation is taken over neighbor pairs in the first, second, and third coordination shells.

We would like to point out that for more accurately MC simulations we should take into account interactions between magnetic atoms located at different coordination shells. The greater the number of coordination shells considered in the MC calculations, the more accurate the transition temperature will be determined. It is followed from the oscillation behavior of the magnetic exchange couplings depended on the distance between atoms. It means that the transition temperature will be the damped oscillation function of the number of coordination shells. The account of interactions in greater coordination shells will result to increase the total exchange parameter $\sum J_0^{\mu\nu}$, hence it leads to higher the transition temperature too. Unfortunately, there is a technical problem in MC method which is related to the computation time if we take into account interactions in greater coordination shells. In the proposed model for numerical simplicity in the MC simulations, we consider interactions between neighbors located until fourth coordination shell. The enhancement of J_{ij} can be achieved by the increasing of mangetoelastic parameters U_{ij}, because as it is followed from Eq. (6), the U_{ij} parameter renormalizes the magnetic exchange interaction.

The normalized magnetization of the 3-6 state Potts model and the strain order parameter of the BEG model are defined in the following way:

$$m = \frac{1}{N}\left(\frac{q_{\mathrm{Ni}}N_{max}^{\mathrm{Ni}} - N_{\mathrm{Ni}}}{q_{\mathrm{Ni}} - 1} + \frac{q_{\mathrm{Mn}}N_{max}^{\mathrm{Mn}} - N_{\mathrm{Mn}}}{q_{\mathrm{Mn}} - 1}\right), \tag{7}$$

$$\varepsilon = \frac{1}{N}\sum_{i}^{N}\sigma_i, \tag{8}$$

where N is the total number of Ni and Mn atoms, q_{Ni} and q_{Mn} are the numbers of magnetic states of Ni and Mn, N_{max}^{Ni} and N_{max}^{Mn} are the maximum numbers of identical magnetic states on the lattice, and N_{Ni} and N_{Mn} are the numbers of Ni and Mn atoms on the lattice, respectively.

The magnetic χ_m and structural χ_ε susceptibilities are defined as

$$\chi_m(T, H_{ext}) = \frac{1}{k_B T}\left[\langle m^2\rangle - \langle m\rangle^2\right], \tag{9}$$

$$\chi_\varepsilon(T, H_{ext}) = \frac{1}{k_B T}\left[\langle \varepsilon^2\rangle - \langle \varepsilon\rangle^2\right]. \tag{10}$$

The magnetocaloric quantities such magnetic specific heat (C_{mag}), magnetic entropy (S_{mag}), isothermal magnetic entropy change (ΔS_{mag}), and adiabatic temperature change (ΔT_{ad}) are derived as in[2,45,46]

$$C_{mag}(T, H_{ext}) = \frac{1}{k_B T^2}\left[\langle \mathcal{H}^2\rangle - \langle \mathcal{H}\rangle^2\right], \tag{11}$$

$$S_{mag}(T, H_{ext}) = \int_{T_1}^{T_2} \frac{C_{mag}(T, H_{ext})}{T} dT, \tag{12}$$

$$\Delta S_{mag}(T, H_{ext}) = S_{mag}(T, H_{ext}) - S_{mag}(T, 0), \tag{13}$$

$$\Delta T_{ad}(T, H_{ext}) = -T\,\frac{\Delta S_{mag}(T, H_{ext})}{C(T, H_{ext})}. \tag{14}$$

Here, $S_{mag}(T, H_{ext})$ and $S_{mag}(T, 0)$ denote the magnetic entropy in presence of a magnetic field H_{ext} and in zero field, respectively. $C(T, H_{ext})$ is the total specific heat $C = C_{mag} + C_{lat}$, where C_{lat} is the lattice heat capacity. For calculation the lattice heat capacity we use standard Debye approximation.[2,45,46] The electronic part of the total specific heat is considered as negligible.

V. RESULTS OF THE MONTE CARLO CALCULATIONS

In this section, we present results of our magnetocaloric simulations for $Ni_2Mn_{0.75}Cu_{0.25}Ga$ alloy with a coupled magnetostructural phase transition using standard Metropolis algorithm.[45] Since we have used the real crystalline lattice, the coordination number of nearest neighbor atoms takes various values for each atom of the cubic and tetragonal unit cells. The number of sites is $N = L^3$, where L is the number of real cubic unit cells of Heusler alloys. Each unit cell consists of 14 Ga, 13 Mn, and 8 Ni atoms.[45,46] We have used $L = 6$, and, for example, in the case of $Ni_2Mn_{0.75}Cu_{0.25}Ga$ the simulation cell contains 824 Mn, 1728 Ni, 274 Cu, and 1099 Ga atoms. The configurations of Cu atoms on the Mn sublattice are chosen randomly, and their total number is fixed by the composition of $Ni_2Mn_{0.75}Cu_{0.25}Ga$. For a given

temperature, the number of MC steps at each site was taken as 5×10^5. The simulation started from the ferromagnetic martensitic phase with $q_{Ni} = 1$, $q_{Mn} = 1$, and $\sigma_i = 1$. In order to obtain equilibrium values of H, m, and ε, the first 10^4 MC steps were discarded. The degeneracy factor p and the Landé factor g were taken as $p = 2$ and $g = 2$. The values of the spin states (i.e., the q_{Ni} and q_{Mn} variable) were taken as corresponding to a such random number r that $0 \le r \le 1$ and the values of q_{Ni} and q_{Mn} were fixed according to the scheme: if $0 \le r \le l/3$, then $q_{Ni} = l$, $l = 1, 2, 3$, and if $0 \le r \le k/6$, then $q_{Mn} = k$, $k = 1 \ldots 6$.

For the calculation of magnetocaloric properties of $Ni_2Mn_{0.75}Cu_{0.25}Ga$, we have used parameters listed in Table II. Here d/a is a function of the distance between atoms in the units of the lattice constant a. The dimensionless magnetoelastic interaction constant is taken as $K_1 = 0.25$.

Approximate values of the structural exchange interaction J, the magnetostructural constants U_{ij} in the austenite and martensite, and K_1 have been taken such as in Ref. 45. The values for the magnetic exchange parameters in the cubic and tetragonal phases have been taken from Fig. 3.

Figure 5(a) shows the theoretical thermomagnetization curves and strain deformations of $Ni_2Mn_{0.75}Cu_{0.25}Ga$ alloy in zero and 1.83 T magnetic fields. As one can see from Fig. 5(a), the calculated normalized magnetization m and strain order parameter ε coincide for various magnetic fields, which points to a coupled magnetostructural phase transition. The coincidence of the maximum values of magnetic and strain susceptibilities, χ_m and χ_ε, falling into the regions of magnetic and structural phase transitions (Fig. 5(b)) also points to a coupled magnetostructural phase transition. It should be noted that the coupled magnetostructural transformation has indeed been observed experimentally in $Ni_2Mn_{0.75}Cu_{0.25}Ga$ alloy.[18,24]

In Fig. 6 we present theoretical and experimental results of MCE for $Ni_2Mn_{0.75}Cu_{0.25}Ga$ upon variation of the magnetic field from 0 to 1.83 and 2 T. Fig. 6(a) contains theoretical and experimental temperature dependence of the isothermal magnetic entropy change ΔS_{mag}. It should be noted that the experimental ΔS_{mag} was calculated from the isothermal magnetization data using thermodynamical Maxwell relation.[19] The inset in Fig. 6(a) represents maximum magnetic entropy changes of $Ni_2Mn_{0.75}Cu_{0.25}Ga$ as a function of the magnetic field.[19] It is seen from the comparison of the theoretical and experimental ΔS_{mag} *vs* T

TABLE II. Model parameters (in meV) for $Ni_2Mn_{0.75}Cu_{0.25}Ga$ alloy.

Parameter	$(c/a = 1)$[a]	$(c/a = 1.147)$[b]
$(d/a \approx 0.7)\, J^m_{Mn-Mn}$	−0.107	3.345
$(d/a \approx 0.76)\, J^m_{Mn-Mn}$		0.314
$(d/a = 1.0)\, J^m_{Mn-Mn}$	1.394	0.429
$(d/a \approx 0.43)\, J^m_{Mn-Ni}$	4.192	
$(d/a \approx 0.45)\, J^m_{Mn-Ni}$		5.029
J	2.0	2.0
U_{ij}	1.5	6.3
K	0.77	0.77

[a]Austenite.
[b]Martensite.

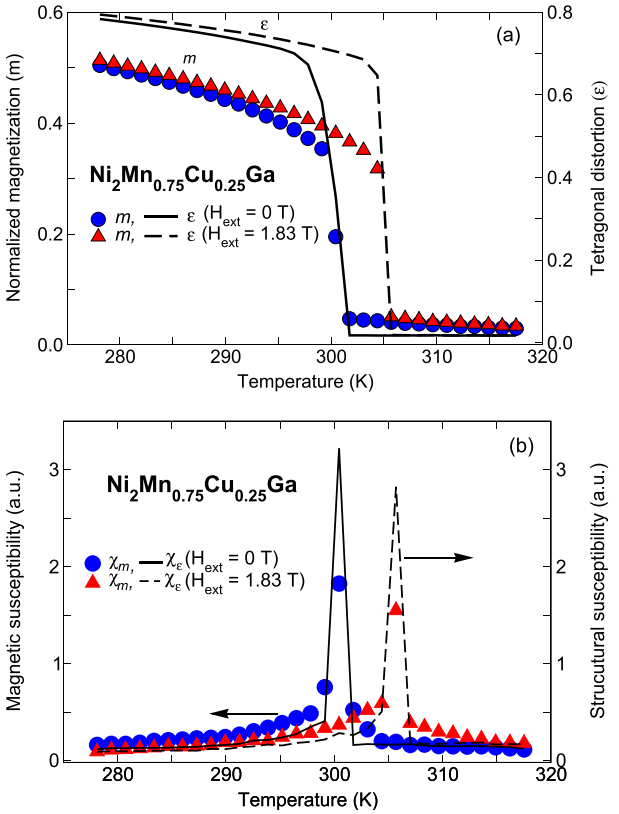

FIG. 5. Calculated temperature dependence of (a) the normalized magnetization m, tetragonal distortion ε, and of (b) the susceptibilities of the magnetic and strain order parameters χ_m and χ_ε, respectively, for $Ni_2Mn_{0.75}Cu_{0.25}Ga$ in a magnetic field of 0 and 1.83 T. Here, filled symbols mark the normalized magnetization m and magnetic susceptibility χ_m, and solid and dashed lines mark the order parameter ε and related strain susceptibility of strain χ_ε.

dependencies that at the magnetostructural phase transition temperature experimental values of ΔS_{mag} are considerably larger than the theoretical ones. We suppose that our results are more accurate because theoretical ΔS_{mag} was calculated from the magnetic specific heat curves whereas experimental ΔS_{mag} was evaluated from the Maxwell relation which frequently overestimates magnitude of MCE for the alloys with coupled magnetostructural phase transitions.

Comparison of theoretical and experimental results for the adiabatic temperature change ΔT_{ad} is shown in Fig. 6(b). The experimental data have been obtained from direct measurements of the MCE (Fig. 1). Theoretical ΔT_{ad} curves were calculated using Eq. (14). One can see that there is a good agreement between theoretical results obtained in the framework of the proposed model and the experimental data.

We would like to point out that for calculation of ΔT_{ad} we used the magnetic part of isothermal entropy change (see Eqs. (11)–(13)). As is well known, in giant MCE materials a strong coupling between magnetic subsystem and crystallographic structure occurs at the phase transition. Recently, Pecharsky *et al.*[48] have reviewed thermodynamics of the MCE, in particular, the giant MCE in materials with the first-order phase transformations. In this case the phase transition is accompanied by enthalpy of the transition ΔE. According to Ref. 48, the entropies at magnetic field H_{ext} ($H_{ext} = 0$ T or $H_{ext} \neq 0$ T) below the phase transition temperature

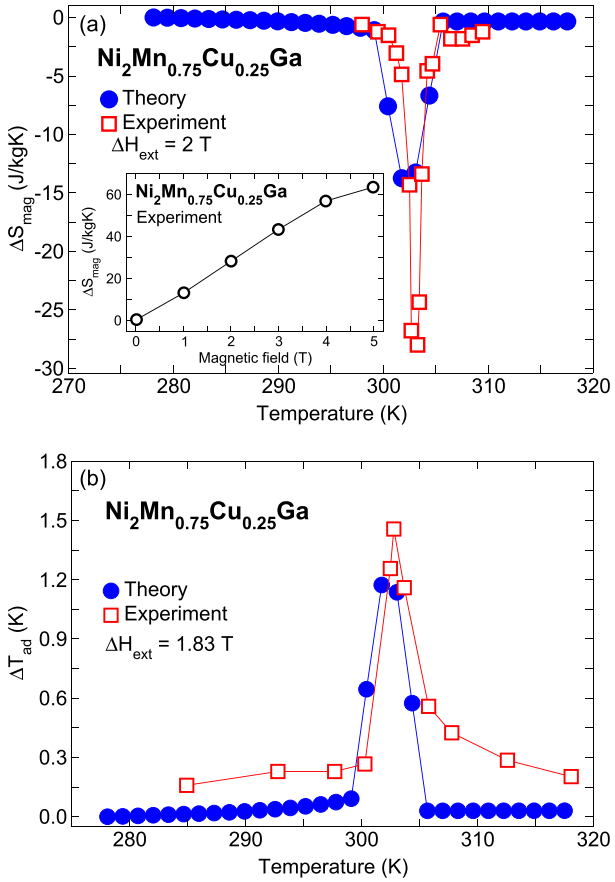

FIG. 6. (a) Theoretical and experimental isothermal magnetic entropy changes in $Ni_2Mn_{0.75}Cu_{0.25}Ga$ for the magnetic field change from 0 to 2 T. The experimental curve was taken from Ref. 19. Shown in the inset is isothermal magnetic entropy change in $Ni_2Mn_{0.75}Cu_{0.25}Ga$ as a function of the magnetic field taken from Ref. 19. (b) Theoretically calculated vs experimentally measured (see Fig. 1) adiabatic temperature change in $Ni_2Mn_{0.75}Cu_{0.25}Ga$ for the magnetic field change from 0 to 1.83 T.

$(T(H_{ext}) < T_m(H_{ext}))$ can be calculated using Eq. (12), whereas in opposite case, $T(H_{ext}) > T_m(H_{ext})$, the entropies should be calculated in form of Eq. (12) with an additional term $\Delta E(H_{ext})/T_m$. It follows from our Monte Carlo simulations that the enthalpy contribution $\Delta E(H_{ext})/T_m$ is 0.64 (0.59) J/mol K (or 2.623 (2.418) J/kg K) in the magnetic field of 0 (1.83) T, respectively. These values were obtained from the temperature dependencies of the internal energy of the system using the total Hamiltonian (Eq. (3)). Taking into account both magnetic and lattice contributions to the entropy change, the adiabatic temperature change ΔT_{ad} was recalculated and it has value of ≈2.56 K. Thus, this value of ΔT_{ad} is approximately two times more than that computed from the magnetic contribution (see Fig. 6(b)). Obviously, the contribution of lattice entropy accounts for 46% of the total MCE. It is can be concluded therefore that the structural contribution plays important role in the enhancement of MCE in materials undergoing coupled first-order magnetostructural phase transformation.

VI. CONCLUSIONS

In this work we have investigated the magnetic and magnetocaloric properties of $Ni_2Mn_{1-x}Cu_xGa$ Heusler alloys by means of first-principles calculations, classical Monte Carlo simulations, and the direct measurements of the magnetocaloric effect. Our calculations of the magnetic exchange parameters have shown that the increase of Copper content in the $Ni_2Mn_{1-x}Cu_xGa$ alloys markedly decreases magnetic interactions between Mn and Ni atoms in the austenitic as well as in the martensitic phase. As for the Mn-Mn interactions, their strength, as well as the tendency to increase or to decrease with the variation of Cu content depends on coordination sphere (Fig. 2). Since the Mn-Ni interactions are the strongest in the stoichiometric Ni_2MnGa, their decrease with the increase of the Cu excess indicates that the degradation of magnetic properties in $Ni_2Mn_{1-x}Cu_xGa$ cannot be ascribed solely to the dilution of the magnetic subsystem.

Developed Monte Carlo model allowed us to simulate accurately magnetocaloric properties of systems undergoing coupled magnetostructural phase transitions. The Monte Carlo calculations of MCE in $Ni_2Mn_{0.75}Cu_{0.25}Ga$ give a reasonable value for the isothermal magnetic entropy change ΔS_{mag} in the vicinity of the magnetostructural phase transition. Although the theoretical ΔS_{mag} is twice smaller than the experimental one (Fig. 6(a)) it should be noted that the accuracy of the experimental method based on the calculation of ΔS_{mag} using the Maxwell relation is rather low in the case of a sharp first-order magnetostructural transition which frequently leads to the significant overestimation of ΔS_{mag}. Considering another characteristic of MCE — the adiabatic temperature change ΔT_{ad} — there is a good agreement between theoretically calculated and experimentally measured ΔT_{ad} (Fig. 6(b)). Since direct measurements of ΔT_{ad} revealed that its magnitude at the magnetostructural transition depends on the measurement protocol (Fig. 1), our choice to compare theoretical data with the ΔT_{ad} *vs* T curve measured upon cooling protocol is motivated by the following simple reasoning. It has been argued in a recent paper[32] that in the case of magnetostructural transition "ferromagnetic martensite ↔ paramagnetic austenite" a contribution of the structural subsystem to MCE under low or moderate magnetic fields can be expected only when MCE is measured upon cooling protocol. Since the magnetostructural interactions is taken into account in our Monte Carlo model (Eq. (3)) it is quite reasonable to compare theoretical ΔT_{ad} with that measured experimentally upon cooling protocol.

ACKNOWLEDGMENTS

This work was supported by RFBR grant Nos. 11-02-00601 and 12-02-31129, RF President Grant MK-6278.2012.2, DFG (SPP 1599), the U.S. Department of Energy (Grant No. DE-FG02-06ER46291), and the Creation and Development Program of NUST "MIS&S." Part of the work was carried out under the Collaborative Research Project of the Institute of Fluid Science, Tohoku University. We thank Professor Peter Entel for discussions regarding the *ab initio* and Monte Carlo techniques.

[1]K. A. Gschneidner, Jr. and V. K. Pecharsky, Int. J. Refrig. **31**, 945 (2008).
[2]A. M. Tishin and Y. I. Spichkin, *The Magnetocaloric Effect and its Applications, IOP Series in Condensed Matter Physics*, edited by J. M. D. Coey, D. R. Tilley, and D. R. Vij (IOP, Bristol, 2003).

[3]A. S. Andreenko, K. P. Belov, S. A. Nikitin, and A. M. Tishin, Sov. Phys. Usp. **32**, 649 (1989).
[4]G. V. Brown, J. Appl. Phys. **47**, 3673 (1976).
[5]K. A. Gschneidner, Jr., V. K. Pecharsky, and A. O. Tsokol, Rep. Prog. Phys. **68**, 1479 (2005).
[6]A. Planes, Ll. Mañosa, and M. Acet, J. Phys.: Condens. Matter **21**, 233201 (2009).
[7]V. D. Buchelnikov and V. V. Sokolovskiy, Phys. Metal. Metall. **112**, 633 (2011).
[8]P. J. Webster, K. R. A. Ziebeck, S. L. Town, and M. S. Peak, Philos. Mag. B **49**, 295 (1984).
[9]V. A. Chernenko, Scr. Mater. **40**, 523 (1999).
[10]A. N. Vasil'ev, V. D. Buchel'nikov, T. Takagi, V. V. Khovailo, and E. I. Estrin, Phys. - Usp. **46**, 559 (2003).
[11]V. V. Kokorin, I. A. Osipenko, and T. V. Shirina, Phys. Metal. Metall. **67**, 173 (1989).
[12]K. Endo, K. Ooiwa, and A. Shinogi, J. Magn. Magn. Mater. **104–107**, 2013 (1992).
[13]V. V. Khovailo, V. A. Chernenko, A. A. Cherechukin, T. Takagi, and T. Abe, J. Magn. Magn. Mater. **272–276**, 2067 (2004).
[14]V. V. Khovaylo, V. D. Buchelnikov, R. Kainuma, V. V. Koledov, M. Ohtsuka, V. G. Shavrov, T. Takagi, S. V. Taskaev, and A. N. Vasiliev, Phys. Rev. B **72**, 224408 (2005).
[15]L. Pareti, M. Solzi, F. Albertini, and A. Paoluzi, Eur. Phys. J. B **32**, 303 (2003).
[16]M. Pasquale, C. P. Sasso, L. H. Lewis, L. Giudici, T. Lograsso, and D. Schlagel, Phys. Rev. B **72**, 094435 (2005).
[17]V. V. Khovaylo, K. P. Skokov, Yu. S. Koshkid'ko, V. V. Koledov, V. G. Shavrov, V. D. Buchelnikov, S. V. Taskaev, H. Miki, T. Takagi, and A. N. Vasiliev, Phys. Rev. B **78**, 060403(R) (2008).
[18]S. Stadler, M. Khan, J. Mitchell, N. Ali, A. M. Gomes, I. Dubenko, A. Y. Takeuchi, and A. P. Guimarães, Appl. Phys. Lett. **88**, 192511 (2006).
[19]M. Khan, S. Stadler, and N. Ali, J. Appl. Phys. **101**, 09C515 (2007).
[20]M. Khan, I. Dubenko, S. Stadler, and N. Ali, J. Appl. Phys. **102**, 023901 (2007).
[21]J. F. Duan, Y. Long, B. Bao, H. Zhang, R. C. Ye, Y. Q. Chang, F. R. Wan, and G. H. Wu, J. Appl. Phys. **103**, 063911 (2008).
[22]B. R. Gautam, I. Dubenko, J. C. Mabon, S. Stadler, and N. Ali, J. Alloys Comp. **472**, 35 (2009).
[23]T. Kanomata, T. Nozawa, D. Kikuchi, H. Nishihara, K. Koyama, and K. Watanabe, Int. J. Appl. Electromagn. Mech. **21**, 151 (2005).
[24]M. Khan, I. Dubenko, S. Stadler, and N. Ali, J. Appl. Phys. **97**, 10M304 (2005).
[25]A. M. Gomes, M. Khan, S. Stadler, N. Ali, I. Dubenko, A. Y. Takeuchi, and A. P. Guimarães, J. Appl. Phys. **99**, 08Q106 (2006).
[26]I. Glavatskyy, N. Glavatska, A. Dobrinsky, J. U. Hoffmann, O. Söderberg, and S. P. Hannula, Scr. Mater. **56**, 565 (2007).
[27]C. Jiang, J. Wang, P. Li, A. Jia, and H. Xu, Appl. Phys. Lett. **95**, 012501 (2009).
[28]M. Kataoka, K. Endo, N. Kudo, T. Kanomata, H. Nishihara, T. Shishido, R. Y. Umetsu, M. Nagasako, and R. Kainuma, Phys. Rev. B **82**, 214423 (2010).
[29]S. Roy, E. Blackburn, S. M. Valvidares, M. R. Fitzsimmons, S. C. Vogel, M. Khan, I. Dubenko, S. Stadler, N. Ali, S. K. Sinha, and J. B. Kortright, Phys. Rev. B **79**, 235127 (2009).
[30]A. T. Zayak, P. Entel, K. M. Rabe, W. A. Adeagbo, and M. Acet, Phys. Rev. B **72**, 054113 (2005).
[31]J. Liu, T. Gottschall, K. P. Skokov, J. D. Moore, and O. Gutfleisch, Nature Mater. **11**, 620 (2012).
[32]V. Khovaylo, "Inconvenient magnetocaloric effect in ferromagnetic shape memory alloys," J. Alloys Compd. (published online).
[33]V. Khovaylo, K. P. Skokov, O. Gutfleisch, H. Miki, R. Kainuma, and T. Kanomata, Appl. Phys. Lett. **97**, 052503 (2010).
[34]H. Ebert, D. Ködderitzsch, and J. Minár, Rep. Prog. Phys. **74**, 096501 (2011).
[35]A. I. Liechtenstein, M. I. Katsnelson, V. P. Antropov, and V. A. Gubanov, J. Magn. Magn. Mater. **67**, 65 (1987).
[36]H. J. Monkhorst and J. D. Pack, Phys. Rev. B **13**, 5188 (1976).
[37]C. G. Broyden, Math. Comp. **19**, 577 (1965).
[38]G. P. Srivastava, J. Phys. A: Math. Gen. **17**, L317 (1984).
[39]W. H. Press, S. A. Teukolsky, W. T. Vetterling, and B. P. Flannery, *Numerical Recipes in Fortran 77: The Art of Scientific Computing*, 2nd ed. (Cambridge University Press, Cambridge, 1992).
[40]S. H. Vosko, L. Wilk, and M. Nusair, Can. J. Phys. **58**, 1200 (1980).
[41]A. G. Khachaturyan, S. M. Shapiro, and S. Semenovskaya, Phys. Rev. B **43**, 10832 (1991).
[42]V. V. Khovaylo, T. Kanomata, T. Tanaka, M. Nakashima, Y. Amako, R. Kainuma, R. Y. Umetsu, H. Morito, and H. Miki, Phys. Rev. B **80**, 144409 (2009).
[43]S. Kaufmann, U. K. Rössler, O. Heczko, M. Wuttig, J. Buschbeck, L. Schultz, and S. Fähler, Phys. Rev. Lett. **104**, 145702 (2010).
[44]E. Şaşioğlu, L. M. Sandratskii, P. Bruno, and I. Galanakis, Phys. Rev. B **72**, 184415 (2005).
[45]V. D. Buchelnikov, V. V. Sokolovskiy, H. C. Herper, H. Ebert, M. E. Gruner, S. V. Taskaev, V. V. Khovaylo, A. Hucht, A. Dannenberg, M. Ogura, H. Akai, M. Acet, and P. Entel, Phys. Rev. B **81**, 094411 (2010).
[46]V. D. Buchelnikov, V. V. Sokolovskiy, S. V. Taskaev, V. V. Khovaylo, A. A. Aliev, L. N. Khanov, A. B. Batdalov, P. Entel, H. Miki, and T. Takagi, J. Phys. D: Appl. Phys. **44**, 064012 (2011).
[47]A. Kimura, S. Suga, T. Shishidou, S. Imada, T. Muro, S. Y. Park, T. Miyahara, T. Kaneko, and T. Kanomata, Phys. Rev. B **56**, 6021 (1997).
[48]V. K. Pecharsky, K. A. Gschneidner, Jr., A. O. Pecharsky, and A. M. Tishin, Phys. Rev. B **64**, 144406 (2001).